The Astrophysical Journal, 594:25–32, 2003 September 1

FUTURE TYPE Ia SUPERNOVA DATA AS TESTS OF DARK ENERGY FROM MODIFIED FRIEDMANN EQUATIONS

Yun Wang,[1] Katherine Freese,[2] Paolo Gondolo,[3] and Matthew Lewis[4]

Received 2003 February 9; accepted 2003 May 14

ABSTRACT

In the Cardassian model, dark energy density arises from modifications to the Friedmann equation, which becomes $H^2 = g(\rho_M)$, where $g(\rho_M)$ is a new function of the energy density. The universe is flat, matter dominated, and accelerating. The distance-redshift relation predictions of generalized Cardassian models can be very different from generic quintessence models, and can be differentiated with data from upcoming pencil beam surveys of Type Ia supernovae such as *Supernova/Acceleration Probe* (*SNAP*). We have found the interesting result that, once Ω_m is known to 10% accuracy, *SNAP* will be able to determine the sign of the time dependence of the dark energy density. Knowledge of this sign (which is related to the weak energy condition) will provide a first discrimination between various cosmological models that fit the current observational data (cosmological constant, quintessence, Cardassian expansion). Further, we have performed Monte Carlo simulations to illustrate how well one can reproduce the form of the dark energy density with *SNAP*. To be concrete we study a class of two-parameter (n, q) generalized Cardassian models that includes the original Cardassian model (parameterized by n only) as a special case. Examples are given of modified polytropic (MP) Cardassian models that fit current supernova and cosmic microwave background data, and prospects for differentiating between MP Cardassian and other models in future data are discussed. We also note that some Cardassian models can satisfy the weak energy condition $w > -1$ even with a dark energy component that has an effective equation of state $w_X < -1$.

Subject headings: cosmological parameters — cosmology: theory — supernovae: general

1. INTRODUCTION

Recent observations of Type Ia supernovae (Riess et al. 1998; Perlmutter et al. 1999) as well as concordance with other observations (including the microwave background and galaxy power spectra) indicate that the universe is accelerating. Many authors have explored a cosmological constant, a decaying vacuum energy (Freese et al. 1987; Peebles & Ratra 1988; Frieman et al. 1995), quintessence (Wang & Steinhardt 1998; Caldwell, Dave, & Steinhardt 1998; Huey et al. 1999), and gravitational leakage into extra dimensions (Deffayet 2001) as possible explanations for such an acceleration. Recently Freese & Lewis (2002) proposed Cardassian expansion as an explanation for acceleration that invokes no vacuum energy whatsoever.[5] In this model the universe is flat and accelerating, and yet consists only of matter and radiation.

In Cardassian models, the Friedmann equation is modified from $H^2 = 8\pi\rho/(3m_{\rm Pl}^2)$ to

$$H^2 = g(\rho_M) \ , \tag{1}$$

where $g(\rho_M)$ is a different function of the energy density, ρ_M contains only matter and radiation (no vacuum), $H = \dot{a}/a$ is the Hubble parameter (as a function of time), and a is the scale factor of the universe. Models with gravitational leakage into extra dimensions also give a modified Friedmann equation that can be cast into the form of equation (1), but with a vacuum component.

The function $g(\rho_M)$ returns to the usual $8\pi\rho_M/(3m_{\rm Pl}^2)$ during the early history of the universe, but takes a different form that drives an accelerated expansion after a redshift $z \sim 1$. Such modifications to the Friedmann equation may arise, e.g., as a consequence of our observable universe living as a three-dimensional brane in a higher dimensional universe (Chung & Freese 2000). Alternatively, such a Friedmann equation may arise if there is dark matter with self-interactions characterized by negative pressure (Gondolo & Freese 2002a, 2002b).

We wish to study the detectability of the altered Friedmann equations by upcoming observations of Type Ia supernovae such as *SNAP*. As discussed in Freese (2003), the redshift-distance relationship predictions for generalized Cardassian models can be quite different from generalized quintessence models. It is the goal of this paper to see how well we can reproduce the correct form of this dark energy density in upcoming experiments.

For concreteness, we investigate a particular version of generalized Cardassian cosmology. However, our results are intended to generalize to any Cardassian cosmology, i.e., to any function $g(\rho_M)$. The particular model we study is meant to illustrate that, generically, modified Friedmann equations can lead to specific detectable predictions in experiments like *SNAP*.

In this paper we study the following generalization of the original Cardassian model:

$$H^2 = \frac{8\pi G}{3}\rho_M\left[1 + \left(\frac{\rho_{\rm Card}}{\rho_M}\right)^{q(1-n)}\right]^{1/q} . \tag{2}$$

[1] Department of Physics and Astronomy, University of Oklahoma, Norman, OK 73019.

[2] Michigan Center for Theoretical Physics, Physics Department, University of Michigan, Ann Arbor, MI 48109; and Kavli Institute for Theoretical Physics, University of California, Santa Barbara, CA 93106.

[3] Department of Physics, Case Western Reserve University, 10900 Euclid Avenue, Cleveland, OH 44106-7079.

[4] Michigan Center for Theoretical Physics, Physics Department, University of Michigan, Ann Arbor, MI 48109.

[5] The name "Cardassian" refers to a humanoid race in Star Trek whose goal is to accelerate expansion of their evil empire. This race looks alien to us and yet is made entirely of matter.

We call this model the "modified polytropic Cardassian" (MP Cardassian)[6] (Gondolo & Freese 2002a, 2002b), where $G = 1/m_{\rm Pl}^2$ is Newton's universal gravitation constant, $\rho_{\rm Card}$ is a characteristic constant energy density, and where we take $n < 2/3$ and $q > 0$. The original power-law Cardassian model corresponds to $q = 1$.

For comparison, we remind the reader of the original power-law Cardassian model that was proposed in Freese & Lewis (2002), which had the following specific form of $g(\rho_M)$:

$$H^2 = \frac{8\pi}{3m_{\rm Pl}^2}\rho_M + B\rho_M^n \quad \text{with} \quad n < \frac{2}{3} \ . \tag{3}$$

This is equivalent to writing

$$H^2 = \frac{8\pi G}{3}\rho_M\left[1 + \left(\frac{\rho_{\rm Card}}{\rho_M}\right)^{1-n}\right] \ . \tag{4}$$

The first term inside the bracket of equations (2) and (4) dominates initially, so that ordinary Friedmann-Robertson-Walker (FRW) behavior takes place throughout the early universe. At a redshift $z_{\rm Card} \sim 1$, the two terms inside the bracket become equal, and thereafter the second term dominates. Once the second term dominates, it drives the universe to accelerate. The energy density at which the two terms become equal is $\rho_{\rm Card} = \rho_0(1 + z_{\rm Card})^3$, where ρ_0 is the matter density today. The MP Cardassian model of equation (2) depends on three parameters: the numbers n and q and the density $\rho_{\rm Card}$. The latter can be traded for the observed matter density $\Omega_m^{\rm obs}$ (see eq. [12] below).

The original power-law Cardassian model gave the same distance-redshift relation as a quintessence model with constant equation of state parameter $w_q = n - 1$. Generalized Cardassian models, on the other hand, give predictions for the distance-redshift relation that can be very different from generic quintessence models. For example, some Cardassian models can satisfy the weak energy condition $w > -1$ even with a dark energy component that has an effective equation of state $w_X = p_X/\rho_X < -1$. Note that an effective $w_X < -1$ is consistent with recent cosmic microwave background (CMB) and large-scale structure data (Schuecker et al. 2003; Melchiorri et al. 2002). In this paper we explore these differences and their testability for the MP Cardassian model.

The Cardassian model also has the attractive feature that matter alone is sufficient to provide a flat geometry. Because of the extra term on the right-hand side of the Friedmann equation, the critical mass density necessary to have a flat universe can be modified, e.g., to 0.3 of the usual value. Hence, the matter density can have exactly this new critical value and satisfy all the observational constraints such as given by the cluster baryon fraction and the galaxy power spectrum.

In a flat universe, the total energy density of the universe can be written as

$$\rho_{\rm total}(z) = \rho_{c,\rm old}[\Omega_m^{\rm obs}(1+z)^3 + \Omega_X f_X(z)] \ . \tag{5}$$

Here, $\Omega_m^{\rm obs}$ is the observed matter density of the universe; we take $\Omega_m^{\rm obs} = 0.3$ as our fiducial value. The critical density of the universe (for the ordinary Friedmann equation) is $\rho_{c,\rm old} = 2 \times 10^{-29}\ h_0^2$ g cm^{-3}, where h_0 is the Hubble constant today in units of 100 km s^{-1} Mpc^{-1}. We take

$$\Omega_X = 1 - \Omega_m^{\rm obs} \tag{6}$$

(for a flat universe with total energy density $\Omega_{\rm tot} = 1$), and $f_X(z = 0) = 1$. The subscript X refers to any component of the universe that provides an additional term in Einstein's equation; generically it is called "dark energy," but in the Cardassian case it is an additional matter term. The dark energy density is

$$\rho_X(z) = \rho_X(0) f_X(z) = \rho_{c,\rm old}\Omega_X f_X(z) \ . \tag{7}$$

If the dark energy density corresponds to a cosmological constant, then one finds that $f_X(z) = 1$ at all redshifts z.

Note that for generalized Cardassian models, *both* terms in equation (5) come from matter;

$$\Omega_m^{\rm tot} = \Omega_m^{\rm obs} + \Omega_X = 1 \ . \tag{8}$$

For the MP generalized Cardassian models of equation (2), the dimensionless dark energy density $f_X(z)$ is given by

$$f_X(z) = \frac{\rho_X(z)}{\rho_X(0)} = \frac{\Omega_m^{\rm obs}(1+z)^3}{1-\Omega_m^{\rm obs}}\left\{\left[1 + \frac{(\Omega_m^{\rm obs})^{-q} - 1}{(1+z)^{3(1-n)q}}\right]^{1/q} - 1\right\} . \tag{9}$$

For fixed $\Omega_m^{\rm obs}$, it depends on the two dimensionless parameters n and q.

In Cardassian models, the observed matter density fraction today is given by the ratio of the critical mass density of the Cardassian universe, $\rho_{c,\rm Card} = \rho_0$, and that of the standard universe, $\rho_{c,\rm old} \equiv 3H_0^2/(8\pi G)$. So the observed matter fraction today in the MP Cardassian model is (Freese & Lewis 2002)

$$\Omega_m^{\rm obs} = \frac{\rho_0}{\rho_{c,\rm old}} = \frac{1}{[1 + (1+z_{\rm Card})^{3q(1-n)}]^{1/q}} \ . \tag{10}$$

Inversely, we can express $z_{\rm Card}$, and $\rho_{\rm Card}$, in terms of $\Omega_m^{\rm obs}$ as

$$1 + z_{\rm Card} = \left[\left(\frac{1}{\Omega_m^{\rm obs}}\right)^q - 1\right]^{1/3q(1-n)} \tag{11}$$

and

$$\rho_{\rm Card} = \rho_{c,\rm old}\Omega_m^{\rm obs}\left[\left(\frac{1}{\Omega_m^{\rm obs}}\right)^q - 1\right]^{1/q(1-n)} \ . \tag{12}$$

First, we compare the MP Cardassian model of equation (2) with existing data from supernovae and cosmic microwave background. Next, we explore how plausible future SN Ia data can be optimally used to constrain dark energy models, and whether generalized Cardassian models can be differentiated from generic models of quintessence and models with a cosmological constant.

Most of this work was performed in 2002 September when all the authors were at the Kavli Institute for Theoretical Physics in Santa Barbara. Subsequent dispersal of all the authors to different parts of the country caused the conclusion of the paper to take a long time.

[6] The name "modified polytropic" arises in the context of treating this model as a fluid; then the relationship between energy density and pressure is roughly polytropic (see Gondolo & Freese 2002a, 2002b).

2. COMPARISON OF MP CARDASSIAN WITH CURRENT DATA

In this section, we compare the modified polytropic Cardassian model of equation (2) with current supernova and CMB data. We show that the existing data can be well fitted for several choices of the parameters n and q.

In a smooth Friedmann-Robertson-Walker (FRW) universe, the metric is given by $ds^2 = dt^2 - a^2(t)[dr^2/(1-kr^2) + r^2(d\theta^2 + \sin^2\theta d\phi^2)]$, where $a(t)$ is the cosmic scale factor, and k is the global curvature parameter. The comoving distance r is given by (Weinberg 1972)

$$r(z) = cH_0^{-1}\frac{S(\kappa\Gamma)}{\kappa}\ , \quad \kappa \equiv |\Omega_k|^{1/2}\ , \tag{13}$$

$$\Gamma(z;\Omega_m^{\rm obs},\Omega_X,F) = \int_0^z dz'\frac{1}{E(z')}\ , \tag{14}$$

$$E(z') \equiv \left[\Omega_m^{\rm obs}(1+z')^3 + \Omega_X f_X(z') + \Omega_k(1+z')^2\right]^{1/2}\ , \tag{15}$$

where $\Omega_k = 1 - \Omega_m^{\rm obs} - \Omega_X$, and

$$S(x) = \begin{cases} \sinh(x)\ , & \Omega_k > 0\ , \\ x\ , & \Omega_k = 0\ , \\ \sin(x)\ , & \Omega_k < 0\ . \end{cases} \tag{16}$$

The angular diameter distance is given by $d_A(z) = r(z)/(1+z)$, and the luminosity distance is given by $d_L(z) = (1+z)r(z)$.

The distance modulus for a standard candle at redshift z is

$$\mu_p(z) \equiv m - M = 5\log\left[\frac{d_L(z)}{\rm Mpc}\right] + 25\ , \tag{17}$$

where m and M are the apparent and absolute magnitudes of the standard candle, and $d_L(z)$ is its luminosity distance. Type Ia supernovae (SNe Ia) are our best candidates for cosmological standard candles, because they can be calibrated to have small scatters in their peak luminosity (Phillips 1993; Riess, Press, & Kirshner 1995).

Figure 1 shows the measured distance modulus (actually the deviation of the distant modulus with respect to the expected values for an open universe with $\Omega_m^{\rm obs} = 0.3$ and $\Omega_\Lambda = 0$) for flux-averaged[7] (Wang 2000b) SN Ia data (Riess et al. 1998; Perlmutter et al. 1999) as a function of redshift. For comparison, superposed on the data points are the predictions for several familiar cosmological models (*dotted curves*), from top to bottom: $(\Omega_m, \Omega_\Lambda) = (0.3, 0.7)$, $(0.3, 0)$, and $(1, 0)$. In addition, three examples of modified polytropic Cardassian models from equation (2) are shown, all with $\Omega_m^{\rm obs} = 0.3$. The three models have parameters $n = 0.2$, $q = 1$ (*solid curve*); $n = 0.2$, $q = 2$ (*short dashed curve*); and $n = 0.2$, $q = 3$ (*long dashed curve*). Note that the solid curve is equivalent to a quintessence model with $w_q = -0.8$. Also shown in Figure 1 is a quintessence model with $w_q(z) = -1 + 0.5z$, for comparison (*dot-dashed line*). All three generalized Cardassian models shown satisfy current constraints from SNe Ia, so we conclude that MP Cardassian models fit the existing supernova data very well.

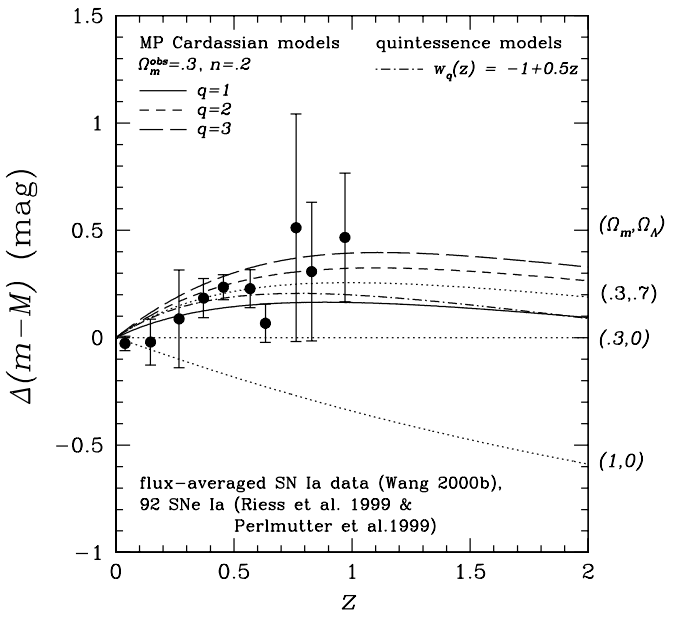

FIG. 1.—Examples of MP Cardassian models (see eq. [2]) that satisfy current observational constraints from Type Ia supernovae (SNe Ia) data. Three MP Cardassian models are shown, all with $\Omega_m^{\rm obs} = 0.3$: $n = 0.2$, $q = 1$ (*solid curve*); $n = 0.2$, $q = 2$ (*short-dashed curve*); and $n = 0.2$, $q = 3$ (*long-dashed curve*). Note that the solid curve is equivalent to a quintessence model with $w_q = -0.8$. The dot-dashed curve is a quintessence model with $w_q = -1 + 0.5z$. The dotted curves show several familiar cosmological models for comparison (from top to bottom): $(\Omega_m, \Omega_\Lambda) = (0.3, 0.7)$, $(0.3, 0)$, and $(1, 0)$.

Figure 2 shows the (n, q) parameter space with constraints from current observational data from both supernovae and the CMB, at a fixed value $\Omega_m = 0.3$. The MP Cardassian model with parameters (n, q) is compared with a fiducial ΛCDM (cold dark matter) model $\Omega_m = 0.3$, $\Omega_b = 0.05$, $\Omega_\Lambda = 0.7$, and $h = 0.65$. The constraints are derived by requiring that the MP Cardassian models agree with the fiducial ΛCDM model to within 1 σ of the measurement uncertainties of the *Wilkinson Microwave Anisotropy Probe* (*WMAP*) CMB data (Bennett et al. 2003) and the current SN Ia data (Riess et al. 1998; Perlmutter et al. 1999; flux-averaged with $\Delta z = 0.05$; see Wang 2000b).

The region between the thick solid lines in Figure 2 corresponds to (n, q) values of the MP Cardassian models that satisfy the current SN Ia data (flux-averaged with $\Delta z = 0.05$) within 1 σ of the fiducial ΛCDM model, i.e., $\Delta\chi^2 = \chi^2_{\rm MPC} - \chi^2_{\Lambda\rm CDM} = 1$. Note that the fiducial ΛCDM model ($\Omega_m = 0.3$, $\Omega_\Lambda = 0.7$, $h = 0.65$) corresponds to $n = 0$, $q = 1$.

[7] Here we briefly describe flux averaging. Because of the inhomogeneous distribution of matter in our universe, the light from perfect standard candles (which all have exactly the same peak luminosity) at a given redshift z will experience different amounts of bending (because of matter inhomogeneity along different lines of sight) before reaching the observer. Hence, even perfect standard candles will be observed to have a non-Gaussian spread in peak luminosity because of gravitational lensing (Frieman 1997; Wambsganss et al. 1997; Holz & Wald 1998; Metcalf & Silk 1999; Wang 1999; Wang, Holz, & Munshi 2002; Munshi & Wang 2003). If this effect is not properly taken into account, the estimated cosmological parameters will be biased, i.e., the estimated mean of the parameters will deviate from the true value of the parameters. Fortunately, the total number of photons from all the standard candles at redshift z should remain unchanged in the presence of gravitational lensing (which only redistributes the photons by bending the light from each standard candle); therefore the average peak luminosity of all the standard candles at z should be the same as the peak luminosity of a standard candle at z *without* gravitational lensing. This is the basic idea behind flux averaging of Type Ia supernova data. For details, see Wang (2000b).

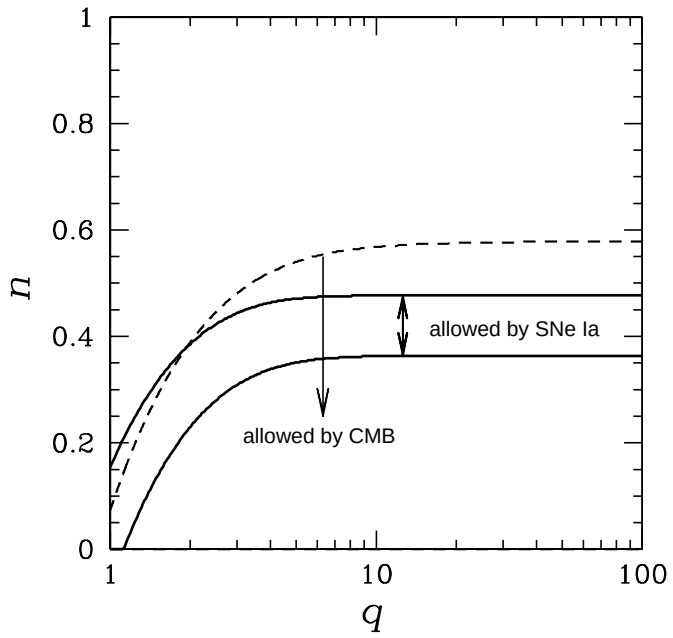

FIG. 2.—Parameter space of (n, q) showing constraints from SNe Ia and CMB at fixed $\Omega_m = 0.3$. All models below the dashed line are in agreement with the shift parameter $\mathscr{R}$ as measured by *WMAP*. All models between the solid lines are in agreement with the SN Ia data.

Complementary plots showing constraints from the power-law Cardassian model with fixed $q = 1$ and varying n and Ω_m are given in Sen & Sen (2003; Zhu & Fujimoto 2002, 2003).

The dashed line in Figure 2 indicates the constraints from *WMAP* CMB data. When the cosmological parameters are varied, the shift in the whole CMB angular spectrum is determined by the shift parameter (Bond, Efstathiou, & Tegmark 1997; Melchiorri et al. 2002; Ödman at el. 2003)

$$\mathscr{R} = \sqrt{\Omega_m} H_0 r(z_{\rm dec}) \ , \tag{18}$$

where $r(z_{\rm dec})$ denotes the comoving distance to the decoupling surface in a flat universe. The results from *WMAP* data require $H_0 r(z_{\rm dec}) = 3.330^{+0.193}_{-0.158}$ and hence give the allowed range in the shift parameter. The corresponding constraints on MP Cardassian model parameters (n, q) are represented by the dashed line in Figure 2. All models in Figure 2 below the dashed line lie within this allowed range for the shift parameter. We conclude that the MP Cardassian models of equation (2) are compatible with current supernova and CMB data.

3. COMPARISON OF MODELS USING SIMULATED FUTURE DATA

In this section, we will construct simulated SN Ia data for three dark energy models: a MP Cardassian model, a cosmological constant model, and a quintessence model. We then investigate if we can recover the original theory from the simulated data. In particular, we want to see if Cardassian cosmology can be differentiated from generic quintessence models or a cosmological constant by analysis of upcoming SN Ia data. We will begin with a modified polytropic Cardassian model of equation (2), choose specific values of the parameters q and n, and see how many SNe Ia we expect.

The measured distance modulus for a SN Ia (labeled "l") is

$$\mu_0^{(l)} = \mu_p^{(l)} + \epsilon^{(l)} \ , \tag{19}$$

where $\mu_p^{(l)}$ is the theoretical prediction (see eq. [17]), and $\epsilon^{(l)}$ is the uncertainty in the measurement, including observational errors and intrinsic scatters in the SN Ia absolute magnitudes. In the simulated data set, we take the dispersion in SN Ia peak luminosity to be $\Delta m_{\rm int} = 0.16$ mag (this is the rms variance of $\epsilon^{(l)}$).

Many (but not all) models of dark energy can be characterized by an equation of state $w_X(z) = p_X(z)/\rho_X(z)$, where $p_X(z)$ is the pressure. Most authors have concentrated on constraining the equation of state w_X of the dark energy from SN data. However, it was shown by Maor, Brustein, & Steinhardt (2001) and Barger & Marfatia (2001) that it is extremely hard to constrain w_X using SN data. Instead, Wang & Garnavich (2001) emphasized that it is easier to extract information on the dark energy density $\rho_X(z)$, instead of $w_X(z)$, from the data. This is because there are multiple integrals relating $w_X(z)$ to the luminosity distance $d_L(z)$ of SNe, which results in a "smearing" that obscures the difference between different $w_X(z)$. It is better to use $\rho_X(z)$ directly, as it is related to the time derivative of the comoving distance to SNe Ia, $r'(z)$; hence, it is less affected by the smearing effect. The advantage of measuring $\rho_X(z)$ over measuring $w_X(z)$ was confirmed by Tegmark (2002). In their work, Wang & Garnavich (2001) assumed that $\rho'_X(z) > 0$, a condition equivalent to the weak energy condition for those cases in which the ordinary Friedmann equation applies. Here, on the other hand, we make no such assumption. In fact, we show that it is possible to determine the sign of $\rho'_X(z)$.

3.1. *Determining the Sign of the Time Dependence of Dark Energy Density, with Prior on* Ω_m

We simulate data for three models (see Table 1): (1) a cosmological constant model; (2) a MP Cardassian model with $n = 0.2$ and $q = 2$, which has $\rho'_X(z) \le 0$; and (3) a quintessence model with $w_X(z) = -1 + 0.5z$, which has $\rho'_X(z) \ge 0$.

Note that MP Cardassian models can have either $\rho'_X(z) \ge 0$ or $\rho'_X(z) < 0$. On the other hand, popular quintessence models in which the quintessence field tracks the matter field have $\rho'_X(z) \ge 0$ (Barger & Marfatia 2001). Figure 3 shows the sign of $\rho'_X(z)$ in the (n, q) parameter space at fixed $\Omega_m = 0.3$ for MP Cardassian models (see eq. [2]) with $\Omega_m^{\rm obs} = 0.3$. The arrows indicate the regions in which $\rho'_X(z) \ge 0$ and $\rho'_X(z) < 0$, respectively. The region in between indicates models with dark energy densities that are *not* monotonic functions of time.

TABLE 1
DARK ENERGY MODELS

Model	Model Parameters	$\rho'_X(z)$
ΛCDM	$\Omega_m = 0.3, \Omega_\Lambda = 0.7$	$\rho'_X(z) = 0$
MP Cardassian model	$\Omega_m^{\rm obs} = 0.3, n = 0.2, q = 2$	$\rho'_X(z) < 0$
Quintessence model	$\Omega_m = 0.3, w_q(z) = -1 + 0.5z$	$\rho'_X(z) \ge 0$

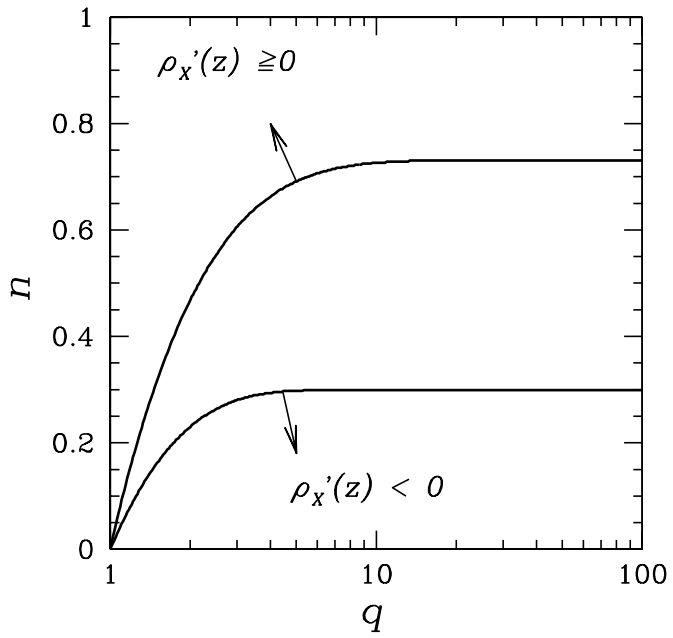

FIG. 3.—Parameter space of (n, q) for MP Cardassian models (see eq. [2]) with $\Omega_m^{\rm obs} = 0.3$. The arrows indicate the regions in which $\rho_X'(z) \geq 0$ and $\rho_X'(z) < 0$, respectively. The region in between indicates models with dark energy densities that are *not* monotonic functions of time.

Note that the weak energy condition requires that the total equation of state $w \geq -1$. In the context of treating Cardassian models as a fluid (Gondolo & Freese 2002a, 2002b), this is

$$w = \frac{p_X}{\rho_m + \rho_X} = -\frac{\left[(\Omega_m^{\rm obs})^{-q} - 1\right]\,(1-n)}{(1+z)^{3(1-n)q} + (\Omega_m^{\rm obs})^{-q} - 1}\ , \qquad (20)$$

which satisfies $w \geq -1$ for the parameter choices we are interested in, $\Omega_m^{\rm obs} < 1$, $n < 1$, and $q > 1$. Therefore, all viable MP Cardassian models satisfy the weak energy condition but can have $w_X < -1$. Note an effective $w_X < -1$ is consistent with recent CMB and large-scale structure data (Schuecker et al. 2003; Melchiorri et al. 2002).

Some scalar field dark energy models with $w_X < -1$ have been studied previously (Caldwell 1999); models that are stable despite violating variants of the weak energy conditions have been found to be difficult to construct (Carroll, Hoffman, & Trodden 2003). Our proposal here is a different alternative to the models previously studied.

We now assume that the data set is given, either from the simulated data sets described above, or in the future from *SNAP*.[8] We show that investigating the data set can reproduce the sign of the time dependence of the dark energy density, assuming one knows the matter density to an accuracy of 10%.

Given our data set, we now proceed as though we have no information on where it comes from; i.e., we proceed as though we did not know which model it came from. We parameterize the dark energy density in order to allow us to compare it to the data set. We take $\rho_X(z)$ to be an arbitrary function. To approximate the function, we parametrize it by its value at $n_{\rm bin}$ equally spaced redshift values, z_i, $i = 1, 2, \ldots, n_{\rm bin}$; $z_{n_{\rm bin}} = z_{\rm max}$. The value of $\rho_X(z)$ at other redshifts are given by linear interpolation, i.e.,

$$\rho_X(z) = \left(\frac{z_i - z}{z_i - z_{i-1}}\right)\rho_{i-1} + \left(\frac{z - z_{i-1}}{z_i - z_{i-1}}\right)\rho_i\ ,$$
$$z_{i-1} < z \leq z_i\ , \quad z_0 = 0\ , \quad z_{n_{\rm bin}} = z_{\rm max}\ . \qquad (21)$$

The values of the dark energy density ρ_i $(i = 1,\ 2, \ldots, n_{\rm bin})$ are the independent variables to be estimated from data; note that the number of independent variables is $n_{\rm bin}$. Again, we proceed as though we had absolutely no information on the function $\rho_X(z)$, and treat it as a completely arbitrary function.

The complete set of parameters, then, is

$$\boldsymbol{s} \equiv (\Omega_m^{\rm obs}\ ,\ \rho_i\ ,\ \text{and}\ n_{\rm bin})\ , \qquad (22)$$

where $i = 1, \ldots, n_{\rm bin}$ as described above. Hence our number of parameters is $N = n_{\rm bin} + 2$. We will vary the number of bins $n_{\rm bin}$ between 1 and 10, and look for the optimal fit to the data. To illustrate, an arbitrary function may become a good approximation to the data for four bins whereas it is a miserable fit for three bins.

We expand the adaptive iteration method developed in Wang & Garnavich (2001) and Wang & Lovelace (2001); unlike what is done in those papers, we do not restrict ourselves to cases in which $\rho_X'(z) > 0$.

We can now determine a best fit to the set of parameters $\boldsymbol{s}$ by using a χ^2 statistic, with (Riess et al. 1998)

$$\chi^2(\boldsymbol{s}) = \sum_l \frac{[\mu_p^{(l)}(z_l|\boldsymbol{s}) - \mu_0^{(l)}(z_l)]^2}{\sigma_l^2}\ , \qquad (23)$$

where $\mu_p^{(l)}(z_l|\boldsymbol{s})$ is the prediction for the distance modulus at redshift z_l, given the set of parameters $\boldsymbol{s}$. Here σ_l is the dispersion of the measured distance modulus due to intrinsic and observational uncertainties in SN Ia peak luminosity.

To reduce the computation time, we can integrate over the Hubble constant H_0 analytically and define a modified χ^2 statistic, with

$$\tilde{\chi}^2 \equiv \chi_*^2 - \frac{C_1}{C_2}\left(C_1 + \frac{2}{5}\ \ln 10\right) - 2\ln\ h^*\ , \qquad (24)$$

where h^* is a fiducial value of the dimensionless Hubble constant h,

$$\mu_p^* \equiv \mu_p(h = h^*) = 42.384 - 5\log h^* + 5\log[H_0 r(1+z)]\ , \qquad (25)$$

and

$$\chi_*^2 \equiv \sum_l \frac{1}{\sigma_l^2}(\mu_p^{*(l)} - \mu_0^{(l)})^2\ ,$$
$$C_1 \equiv \sum_l \frac{1}{\sigma_l^2}(\mu_p^{*(l)} - \mu_0^{(l)})\ ,$$
$$C_2 \equiv \sum_l \frac{1}{\sigma_l^2}\ . \qquad (26)$$

It is straightforward to check that the derivative of $\tilde{\chi}^2$ with respect to h^* is zero; hence, our results are independent of the choice of h^*. We take $h^* = 0.65$.

[8] Note that the current *SNAP* design is substantially improved (Tarle et al. 2003). Here we assume that *SNAP* will obtain all SNe Ia in its survey fields up to $z = 1.7$, similar to a supernova pencil-beam survey (Wang 2000a; Wang & Lovelace 2001).

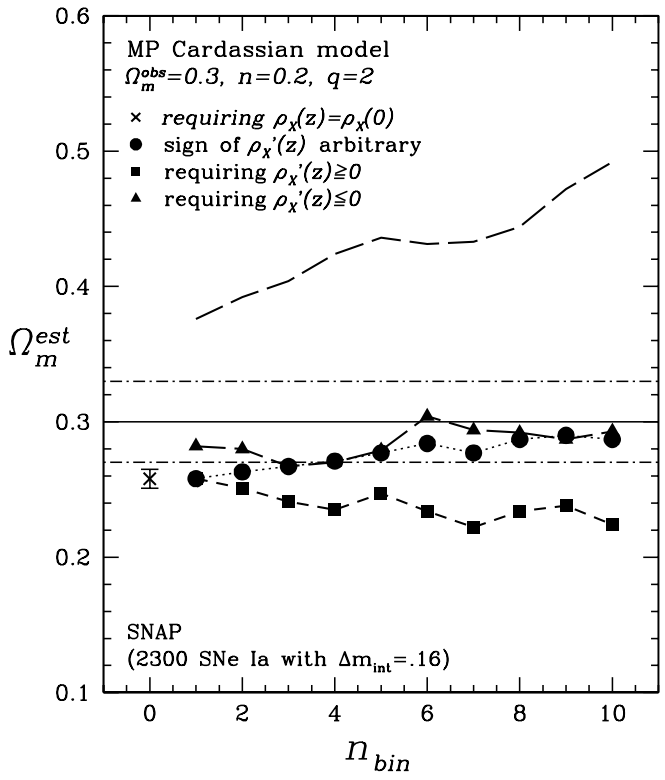

FIG. 4*a*

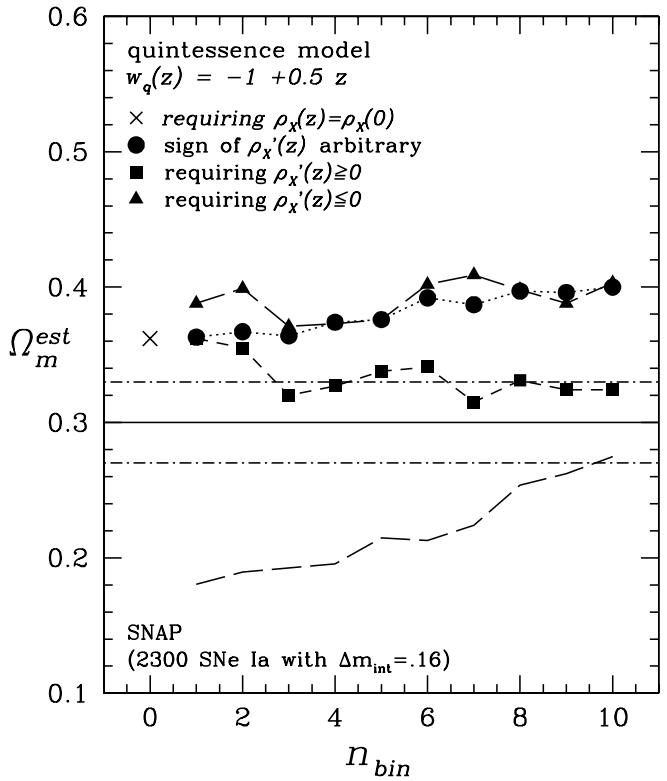

FIG. 4*b*

FIG. 4.—This figure shows that we can, indeed, determine the sign of the dependence of the dark energy density $\rho_X'(z)$; i.e., we can determine if it is increasing, decreasing, or constant in time. The axes show estimated $\Omega_m^{\rm est}$ as function of $n_{\rm bin}$ from the simulated data for *SNAP* for (*a*) a MP Cardassian model with $n = 0.2$ and $q = 2$ so that $\rho_X'(z) < 0$ and (*b*) a quintessence model with $w_X(z) = -1 + 0.5z$ so that $\rho_X'(z) > 0$. The horizontal dot-dashed lines correspond to a 10% uncertainty on $\Omega_m^{\rm obs} = 0.3 \pm 0.03$. The different curves show the results obtained assuming a variety of constraints on the time dependence $\rho_X'(z)$ as labeled. The long-dashed curve shows $\chi^2_{\rm pdf}$ on an arbitrary scale. By requiring the results to lie within the dot-dashed lines, we recover the sign of the time dependence of $\rho_X(z)$.

For a given choice of $n_{\rm bin}$, we can minimize the modified χ^2 statistic of equation (24) to find the best-fit $\Omega_m^{\rm obs}$ and $\rho_X(z)$ (parameterized by ρ_i, $i = 1, 2, \ldots, n_{\rm bin}$).

For each model in Table 1, we obtain *four* sets of best-fit parameters. We apply four different constraints to the arbitrary function $\rho_X(z)$ in order to discover which one allows a good fit. The four constraints are (1) $\rho_X(z) = \rho_X(0) =$ constant; i.e., a cosmological constant model; (2) $\rho_X'(z) \geq 0$; (3) $\rho_X'(z) < 0$; and (4) completely unconstrained $\rho_X(z)$. For each of these constraints, we find the best-fit parameters.

Figure 4 shows our results: Figures 4*a* and 4*b* correspond to the MP Cardassian and quintessence models described in Table 1, respectively. For simulated data of model 1 of Table 1, a cosmological constant model, we find that $\Omega_m^{\rm obs}$ is estimated correctly to 1% accuracy, regardless of the assumption made about $\rho_X'(z)$. For model 2 (MP Cardassian) and model 3 (quintessence), Figures 4*a* and 4*b* show the best-fit $\Omega_m^{\rm obs}$, under all of the four constraints above, for $n_{\rm bin}$ values ranging from 1 to 10. We find that assuming the wrong sign for $\rho_X'(z)$ leads to an estimated Ω_m that differs from the assumed $\Omega_m^{\rm obs}$ by more than 10%. The different constraints on the sign of $\rho_X'(z)$ are represented by different point types. The solid horizontal line is our fiducial value of $\Omega_m = 0.3$ (i.e., we are assuming that this is the true value of the matter density), and the dot-dashed horizontal lines indicate 10% error bars about this fiducial value. We are assuming that Ω_m is known to within 10% from other data sets.

These plots are *not* intended to emphasize the dependence of $\Omega_m^{\rm obs}$ on $n_{\rm bin}$. Indeed, as discussed above, the reason that we have found the best fit Ω_m for a variety of $n_{\rm bin}$ values is simply that the parametrization of the arbitrary function $\rho_X(z)$ may be poor for one value of $n_{\rm bin}$ but excellent for another; we take a given model to be a good one if it lies within the 10% range on Ω_m for several values of $n_{\rm bin}$.

Figures 4*a* and 4*b* show estimated $\Omega_m^{\rm obs}$ as function of $n_{\rm bin}$ for model 2 (MP Cardassian model) and model 3 (a quintessence model). In Figure 4*a*, only the $\Omega_m^{\rm obs}$ values estimated assuming that $\rho_X'(z) \leq 0$ consistently (i.e., for most values of $n_{\rm bin}$) lie within 10% of the true value of $\Omega_m^{\rm obs} = 0.3$. Hence, we have indeed recovered the correct general time dependence of the model underlying this set of simulated data. In Figure 4*b*, only the $\Omega_m^{\rm obs}$ values estimated assuming that $\rho_X'(z) \geq 0$ deviate by less than 10% from the true value of $\Omega_m^{\rm obs} = 0.3$. Again, we have recovered the correct general time dependence of the model underlying this set of simulated data. For all three models, we have been able to correctly ascertain the sign of $\rho_X'(z)$ with this technique.

This indicates that the estimated $\Omega_m^{\rm obs}$ (for a variety of values of $n_{\rm bin}$), together with a 10% accurate prior on $\Omega_m^{\rm obs}$, can be used to determine the general time-dependence of the dimensionless dark energy density, i.e., the sign of $\rho_X'(z)$.

3.2. *Estimating Dark Energy Density from Data*

In this section we create a large number of Monte Carlo samples to see how well we can reconstruct the entire

function $\rho_X(z)$. To create these samples, we need first to identify the best-fit model as follows.

For a given data set, we choose the best-fit model with $n_{\rm bin}$ [the number of parameters used to parametrize the dimensionless dark energy density $\rho_X(z)$] that satisfies the following three conditions:

1. It corresponds to an estimated Ω_m value that deviates less than 10% from the true value.
2. As we decrease $n_{\rm bin}$ from a large value, say, $n_{\rm bin} = 10$, it minimizes the χ^2 per degree of freedom, $\chi^2_{\rm pdf} = \chi^2/(N_{\rm data} - \nu)$, without significantly shifting the estimated value of Ω_m (Wang & Lovelace 2001). Here $N_{\rm data}$ is the number of SNe Ia, and ν is the number of parameters estimated from data. Long dashed lines in Figure 4 show $\chi^2_{\rm pdf}$ as function of $n_{\rm bin}$ on an arbitrary scale.[9]
3. If $\rho'_X(z) \neq 0$, then $n_{\rm bin} > 1$.

Now we apply the above conditions to Figures 4*a* and 4*b*. In Figure 4*a*, as we decrease $n_{\rm bin}$ from $n_{\rm bin} = 10$, the significant shifting in the estimated Ω_m occurs at $n_{\rm bin} = 6$, which also has the smallest $\chi^2_{\rm pdf}$ for $6 \leq n_{\rm bin} \leq 10$. We find that for the MP Cardassian model, *SNAP* data yield an optimal $n_{\rm bin} = 6$. In Figure 4*b*, as we decrease $n_{\rm bin}$ from $n_{\rm bin} = 10$, the significant shifting in the estimated Ω_m occurs at $n_{\rm bin} = 3$, which also has the smallest $\chi^2_{\rm pdf}$ for $3 \leq n_{\rm bin} \leq 10$. Hence, for the quintessence model, *SNAP* data yield an optimal $n_{\rm bin} = 3$.

To derive the error distribution of estimated parameters $\Omega_m^{\rm obs}$ and ρ_i ($i = 1, 2, \ldots, n_{\rm bin}$; see eq. [21]), we create 10^4 Monte Carlo samples by adding dispersion in peak luminosity of $\Delta m_{\rm int} = 0.16$ mag to the distance modulus $\mu_p(z)$ (see eq. [17]) predicted by the best-fit model (i.e., assuming that the best-fit model is the true model). This is equivalent to making 10^4 new "observations," each similar to the original data set (Press et al. 1992). The same analysis used to obtain the best-fit model from the data is performed on each Monte Carlo sample. We use the distribution of the resulting estimates of the parameters ($\Omega_m^{\rm obs}$ and ρ_i) to derive the mean and 68.3% and 99.73% confidence level intervals of the estimated parameters. Wang & Lovelace (2001) showed that such a Monte Carlo analysis gives less biased estimates of parameters than a maximum-likelihood analysis; i.e., the Monte Carlo mean of estimated parameters deviate less from the true values of the parameters.

Figure 5 shows the estimated dimensionless dark energy density $\rho_X(z)$ for a generalized Cardassian model with $n = 0.2$ and $q = 2$ from simulated SN data from *SNAP* assuming that we know Ω_m to 10% accuracy. The solid line indicates the underlying true model for $\rho_X(z)$. The horizontal dashed line near the top of the figure indicates $\rho_X(z) = \rho_X(0) =$ constant, a cosmological constant model. The horizontal dotted line near the bottom of the figure indicates $\rho_X(z) = 0$. We impose $\rho_X(z) \geq 0$. The estimated Ω_m values (obtained by reconstructing the model from the Monte Carlo samples) are listed at the bottom of the plot with 68.3% confidence level intervals. Where the actual value of Ω_m for the fake data set was $\Omega_m = 0.3$, we see that the reproduced Ω_m from our Monte Carlo study is $\Omega_m = 0.298^{+0.024}_{-0.023}$. Indeed, this reproduced value lies within 10% of the correct Ω_m.

The error bars of the reproduced estimates of $\rho_X(z)$ have been computed using 10^4 Monte Carlo random samples derived from the simulated data. The solid error bars and the dotted error bars indicate the 68.3% and 99.73% confidence level intervals, respectively. Hence, from Figure 5, we see that a MP Cardassian model with a set of parameters that fit the current observational data, $\Omega_m^{\rm obs} = 0.3$, $n = 0.2$, $q = 2$, can be differentiated from a cosmological constant model at 99.73% confidence level. We have shown the accuracy with which one can reconstruct the form of the dark energy density. We see that *SNAP* can indeed differentiate between different models.

[9] The scale is adjusted for the curve to fit in the figure.

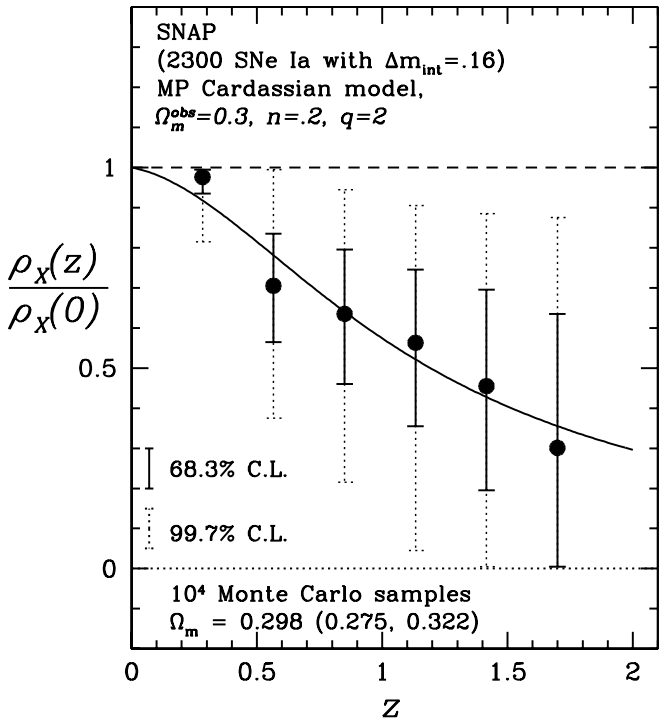

FIG. 5.—Estimated dimensionless dark energy density $\rho_X(z)$ for simulated SN data from *SNAP*, assuming that we know Ω_m to ~10% accuracy (and the correct general time dependence of the dark energy density; see discussion in § 3). The error bars of the estimated $\rho_X(z)$ have been computed from 10^4 Monte Carlo random samples derived from the simulated data. The solid error bars and the dotted error bars indicate the 68.3% and 99.73% confidence level intervals, respectively. The reproduced estimates of Ω_m values are listed at the bottom of the plot with 68.3% confidence level intervals.

4. DISCUSSION AND CONCLUSION

We have compared a particular form of Cardassian model, the modified polytropic Cardassian model of equation (2), with existing data from supernova and cosmic microwave background measurements. We have found that current data constrain the parameter space of the MP Cardassian model.

We have shown that future Type Ia supernova (SN Ia) data from *SNAP* can differentiate various dark energy models (cosmological constant, quintessence, and generalized Cardassian expansion), assuming that Ω_m is known to 10% accuracy. We have found the interesting result that the sign of the time dependence of the dark energy density can be determined by *SNAP*.

Further, we have performed Monte Carlo samples to illustrate how well one can reproduce the form of the dark

energy density with *SNAP*. For example, a MP Cardassian model with a set of parameters that fit the current observational data, $\Omega_m^{\rm obs} = 0.3$, $n = 0.2$, $q = 2$, can be differentiated from a cosmological constant model at 99.73% confidence level.

We wish to remark on another test of generalized Cardassian models. There are two independent motivations for these models: (1) they may arise as a consequence of imbedding our observable universe as a 3-brane in higher dimensions (see, e.g., Chung & Freese 2000), and (2) these models may be described in terms of a fluid interpretation, in which the dark energy density may be due to self-interaction of dark matter particles (Gondolo & Freese 2002a, 2002b). In this second interpretation, we have developed a fully relativistic treatment of the resultant modified Euler's equations, Poisson equations, and energy conservation. Then we analyzed (Gondolo & Freese 2002a, 2002b) the linear growth of density fluctuations in the fluid interpretation. A more complete study of perturbation growth is in progress. Of particular interest is the study of the integrated Sachs-Wolfe effect in the CMB. It is possible that the deficit of power on large angular scales (low-order multipoles) may be explained in generalized Cardassian models.

We thank the Kavli Institute for Theoretical Physics at the University of California, Santa Barbara, for hospitality. Most of this work was performed in 2002 September when all the authors were at the Institute for Theoretical Physics in Santa Barbara. Subsequent dispersal of all the authors to different parts of the country caused a delay in the publication of this paper. It is a pleasure for us to thank Arlin Crotts, Greg Tarle, the referee, and especially Josh Frieman for helpful comments. This research was supported in part by the National Science Foundation under grant PHY 99-07949, NSF CAREER grant AST-0094335 (Y. W.), the Department of Energy grant at the University of Michigan (K. F. and M. L.), and the Michigan Center for Theoretical Physics (K. F. and M. L.). K. F. thanks the Aspen Center for Physics, where part of this research was conducted, for hospitality during her stay.

REFERENCES

Barger, V., & Marfatia, D. 2001, Phys. Lett. B, 498, 67
Bennett, C. L., et al. 2003, ApJS, 148, 1
Bond, J. R., Efstathiou, G., & Tegmark, M. 1997, MNRAS, 291, L33
Caldwell, R. 1999, Phys. Lett. B, 545, 23
Caldwell, R., Dave, R., & Steinhardt, P. 1998, Phys. Rev. Lett., 80, 1582
Carroll, S. M., Hoffman, M., & Trodden, M. 2003, preprint (astro-ph/0301273)
Chung, D. J., & Freese, K. 2000, Phys. Rev. D, 61, 023511
Deffayet, C. 2001, Phys. Lett. B, 502, 199
Freese, K. 2003, in Conf. Proc. for Meeting on Sources and Detection of Dark Matter and Dark Energy in the Universe, in press
Freese, K., Adams, F. C., Frieman, J. A., & Mottola, E. 1987, Nucl. Phys. B, 287, 797
Freese, K., & Lewis, M. 2002, Phys. Lett. B, 540, 1
Frieman, J., Hill, J., Stebbins, A., & Waga, I. 1995, Phys. Rev. Lett., 75, 2077
Frieman, J. A. 1997, Comments Astrophys., 18, 323
Gondolo, P., & Freese, K. 2002a, preprint (hep-ph/0209322)
———. 2002b, preprint (hep-ph/0211397)
Holz, D. E., & Wald, R. M. 1998, Phys. Rev. D, 58, 063501
Huey, G., Wang, L., Dave, R., Caldwell, R., & Steinhardt, P. 1999, Phys. Rev. D, 59, 063005
Maor, I., Brustein, R., & Steinhardt, P. J. 2001, Phys. Rev. Lett., 86, 6 (erratum 87, 049901)
Melchiorri, A., Mersini, L., Ödman, C. J., & Trodden, M. 2002, preprint (astro-ph/0211522)
Metcalf, R. B., & Silk, J. 1999, ApJ, 519, L1
Munshi, D., & Wang, Y. 2003, ApJ, 583, 566
Ödman, C. J., Melchiorri, A., Hobson, M. P., & Lasenby, A. N. 2003, Phys. Rev. D, 67, 083511
Peebles, P. J. E., & Ratra, B. 1988, ApJ, 325, L17
Perlmutter, S., et al. 1999, ApJ, 517, 565
Phillips, M. M. 1993, ApJ, 413, L105
Press, W. H., Teukolsky, S. A., Vetterling, W. T., & Flannery, B. P. 1992, Numerical Recipes in Fortran 77: The Art of Scientific Computing (2d ed.; Cambridge: Cambridge Univ. Press)
Riess, A. G., Press, W. H., & Kirshner, R. P. 1995, ApJ, 438, L17
Riess, A. G., et al. 1998, AJ, 116, 1009
Schuecker, P., et al. 2003, A&AS, 402, 53
Sen, S., & Sen, A. A. 2003, ApJ, 588, 1
Tarle, G., et al. 2003, Proc. SPIE, 4850, 919
Tegmark, M. 2002, Phys. Rev. D, 66, 103507
Wambsganss, J., Cen, R., Xu, G., & Ostriker, J. P. 1997, ApJ, 475, L81
Wang, L., & Steinhardt, P. 1998, ApJ, 508, 483
Wang, Y. 1999, ApJ, 525, 651
———. 2000a, ApJ, 531, 676
———. 2000b, ApJ, 536, 531
Wang, Y., & Garnavich, P. 2001, ApJ, 552, 445
Wang, Y., Holz, D.E., & Munshi, D. 2002, ApJ, 572, L15
Wang, Y., & Lovelace, G. 2001, ApJ, 562, L115
Weinberg, S. 1972, Gravitation and Cosmology (New York: Wiley)
Zhu, Z., & Fujimoto, M. 2002, ApJ, 581, 1
———. 2003, ApJ, 585, 52